Atmos. Chem. Phys. Discuss., 12, 11245–11274, 2012
www.atmos-chem-phys-discuss.net/12/11245/2012/
doi:10.5194/acpd-12-11245-2012

Atmospheric Chemistry and Physics Discussions

The distribution of snow black carbon observed in the Arctic and compared to the GISS-PUCCINI model

T. Dou[1,2,3], C. Xiao[2,3], D. T. Shindell[4], J. Liu[5], J. Ming[2,6], and D. Qin[2]

[1]College of Resources and Environment, Graduate University of Chinese Academy of Sciences, Beijing 100049, China
[2]State Key Laboratory of Cryospheric Sciences, Cold and Arid Regions Environmental and Engineering Research Institute, Chinese Academy of Sciences, Lanzhou 730000, China
[3]Institute of Climate System, Chinese Academy of Meteorological Sciences, Beijing 100081, China
[4]NASA Goddard Institute for Space Studies and Columbia Earth Institute, Columbia University, New York, NY 10025, USA
[5]State Key Laboratory of Numerical Modeling for Atmospheric Sciences and Geophysical Fluid Dynamics, Institute of Atmospheric Physics, Chinese Academy of Sciences, Beijing 100029, China
[6]National Climate Center, China Meteorological Administration, Beijing 100081, China

Received: 21 February 2012 – Accepted: 20 April 2012 – Published: 3 May 2012

Correspondence to: T. Dou (doutf@cams.cma.gov.cn)

Published by Copernicus Publications on behalf of the European Geosciences Union.

ACPD

12, 11245–11274, 2012

Abstract

In this study, we focus on the latest NASA GISS composition-climate model to evaluate its performance in simulating the spatial distribution of snow BC (sBC) in the Arctic relative to present observations. The radiative forcing due to BC deposition to the Arctic snow and sea ice is also estimated. Two sets of model simulations have been done in the analysis, where meteorology is linearly relaxed towards National Centers for Environmental Prediction (NCEP) and towards NASA Modern Era Reanalysis for Research and Applications (MERRA) reanalyses. Results indicate that both of the modeled sBC are in good agreement with present-day observations in and around the Arctic Ocean, except for underestimation at a few sites in the Russian Arctic. The overall ratio of observed to modeled sBC is 1.1. The result from the NCEP run is slightly better than that from the MERRA run. This suggests that the latest GISS-E2-PUCCINI model does not have significant biases in its simulated spatial distribution of BC deposition to the Arctic, and underestimation of biomass burning emissions in Northern Eurasia is preliminarily considered to be the main cause of the simulation biases in the Russian Arctic. The combination of observations and modeling provides a comprehensive distribution of sBC over the Arctic. On the basis of this distribution, we estimate the decrease in snow and sea ice albedo and the resulting radiative forcing. It is concluded that the averaged decrease in snow and sea ice albedo in and around the Arctic Ocean (66–90° N) due to BC deposition is 0.4–0.6 % from spring 2007–2009, leading to regional surface radiative forcings of 0.7 $W m^{-2}$, 1.1 $W m^{-2}$ and 1.0 $W m^{-2}$, respectively in spring 2007, 2008 and 2009.

1 Introduction

Emissions of black carbon (BC) particles result from incomplete combustion during the burning of biomass and fossil fuels, and are considered a significant climate forcing (IPCC, 2007; McConnell et al., 2007). In the atmosphere, the absorption of sunlight

ACPD
12, 11245–11274, 2012

by BC contributes to global warming and alters cloud-formation processes (Jacobson, 2001). After deposition onto snow and ice, BC has the potential to significantly reduce the surface albedo, hence perturbing the radiative balance and possibly leading to earlier snowmelt (Hegg et al., 2009). The average radiative forcing from BC by altering surface albedo was estimated as $+0.1\,W\,m^{-2}$ (IPCC, 2007), with estimates varying from 0.01 to $0.16\,W\,m^{-2}$ (Flanner et al., 2007; Hansen et al., 2004, 2007; Koch et al., 2009a).

Arctic climate is especially vulnerable to BC deposition because of the abundant and wide distribution of relatively clean sea ice, snow and glaciers, which can be impacted effectively by accelerating melting and snow/ice albedo feebacks (McConnell et al., 2007; Koch et al., 2005). Recent research suggests that the seasonally averaged surface forcing by BC in the Arctic can be up to $+0.5\,W\,m^{-2}$ in spring (Flanner et al., 2007; Quinn et al., 2008). The comparisons between model simulations and aerosol BC (aBC) observed in Barrow, Alert and Zeppelin stations and some points of sBC have shown that most previous models underpredict BC in the Arctic, especially in winter and spring (Flanner et al., 2007; Shindell et al., 2008; Koch et al., 2009b; Huang et al., 2010a; Liu et al., 2011). However, the seasonal cycle and magnitude of other trace species, like CO and ozone, are reproduced much better in most models (Shindell et al., 2008).

It is still controversial what are the dominant causes of the present discrepancy between models and observations. Several factors had been suggested, such as the emission inventory used in the model (Wang et al., 2011), modeled transport processes (Liu et al., 2011), the possibility that too few observation sites have been available to adequately validate models, or that challenges in BC measurement methods have biased the observed BC concentrations (Shindell et al., 2008; Doherty et al., 2010). In recent years, model simulations and measurement methods have been updated and greatly improved, so that it is useful to collate comprehensive pan-Arctic sBC observations from previous campaigns to revaluate the current models. Koch et al. (2009b) compared vertical profiles of aBC from several models to aircraft observations during

ACPD
12, 11245–11274, 2012

the International Polar Year (IPY), and suggested that current models underestimated BC concentrations throughout much of the troposphere in different degrees. There still exist large uncertainties in this comparison, because the observations of vertical profiles of aBC just present a "snapshot" of the BC distribution in limited sites, they are not representative over the whole Arctic, especially at climate scales. More extensive and long term observations are still needed to give a comprehensive validation to current models. This study focuses on the latest NASA GISS composition-climate model to investigate how it performs in the simulation of spatial distribution of BC deposition to the Arctic snow and ice. We summarize BC measurements reported to date and add the observations obtained in the 1st Korean Arctic cruise (2010) to the analysis. We use these to evaluate the modeled distribution of sBC in the Arctic and then give a comprehensive map of the spring sBC in and around the Arctic Ocean with a combination of observations and validated model results. Finally, we estimate the decrease in snow and sea ice albedo and resulting radiative forcing due to BC depsotion based on the given sBC distribution.

2 Observations

The earliest observations of sBC mainly started from the mid-1980s (Clarke and Noone, 1985; Cachier, 1997; Slater et al., 2002; Flanner et al., 2007; Forsstrom et al., 2009), and were carried out at only a few sites, such as Camp Century, Greenland (77.2° N, 61.1° W), Dye 3, Greenland (65.2° N, 43.8° W), Alert (83.5° N, 62.5° W), Barrow (71.3° N, 156.6° W) and several Arctic Ocean sites. Later, the spatial distribution of BC in snow and sea ice was investigated during the SHEBA experiment (Grenfell and Sturm, 2002). During recent years, the circumpolar regions were surveyed as a whole, expanding and updating the previous observations (Doherty et al., 2010; Forsstrom et al., 2009), which includes near one hundred sites and two thousand samples in the Arctic and sub-Arctic regions.

ACPD
12, 11245–11274, 2012

We summarize the spring measurements of present-day (from 1998 to 2009) sBC in the Arctic from all studies known to us. Some of these include vertically-integrated measurements or measurements at various depths throughout the snow cover, and others just include surface measurements. Concentrations reported by Doherty et al. (2010) were increased by 11 % to correct for a low bias in the previous data analysis. As reported by Doherty et al. (2010), the vertical distribution of sBC in the Russian Arctic is non-uniform, with larger values in the upper 25 % of the snowpack at most measurement sites (left panel in Fig. 1). In contrast, the concentrations observed in the Canadian Arctic are smaller and relatively uniform throughout the snowpack (right panel in Fig. 1). The two sets of vertical profiles both involve measurements from dozens of snow pits, thus they are considered to be largely representative of the typical distribution of spring sBC in these regions. We calculate the surface and subsurface concentrations of sBC from the observations at different depths, and then derive an empirical formula for estimating the integrated-layer concentration (C_h, $h = h1 + h2$) of sBC. In the case of surface sBC > subsurface sBC:

$$C_h = \frac{25\%\rho_{h1}C_{h1} + 75\%\rho_{h2}C_{h2}}{25\%\rho_{h1} + 75\%\rho_{h2}} \quad (1)$$

where C_{h1} is the concentration of sBC in the surface snow ($h1 = 25\% \cdot h$) at each site, ρ_{h1} is the average density of surface snow, C_{h2} is the concentration of sBC in subsurface ($h2 = 75\% \cdot h$), ρ_{h2} is the average density of subsurface snow and h1 and h2 are as given in Fig. 1. Because there are not observations of snow density that correspond to sBC measurements in various depths, it's impossible to calculate the actual and precise C_h of each site at present. In this study, we apply the estimated snow density of the surface and subsurface layer: $\rho_{h1} = 0.256\,\mathrm{g\,cm^{-3}}$ and $\rho_{h2} = 0.345\,\mathrm{g\,cm^{-3}}$ that is calculated from the mean values of snow density in different types of snow layers observed in the SHEBA campaign (Sturm et al., 2002). These two values of snow layer density are consistent with the typical vertical distribution of spring snow in the Arctic that is generally composed of wind slab, recent and new snow, fine-grained snow, wind

ACPD
12, 11245–11274, 2012

slab, and depth hoar from top to bottom by turns (Sturm et al., 2002). In the estimation of total-layer sBC, we presume that the uncertainties are entirely brought on by the standard deviations of observed snow densities. When surface sBC ≈ subsurface sBC, we take the depth-weighted average of the concentration values in each layer as the estimated vertically-integrated concentration. All of the surface and subsurface observations used in this study and the derived vertically-integrated values are illustrated as Fig. 2.

In order to avoid too much influence from the surrounding urban environment, Table 1 only includes the estimated values of sBC in the Arctic Ocean and its adjacent coastal regions, not including ones far away from the Arctic Ocean. The vertically-integrated values larger than 70 ng g^{-1} have not been applied in this study because of too large difference between surface and subsurface concentrations shown in these sites, which may bring great uncertainties. The sBC concentrations listed in Table 1 have been measured either by the "spectrophotometry" method (for most of the values) (Doherty et al., 2010) or the "thermo-optical" method (Ming et al., 2008). Both of the methods discriminate BC and non-BC fractions of absorption in the measuring process. It is generally thought that the "spectrophotometry" method is better in the albedo effect analysis. However, in spatial distribution analysis, both of them could imply real variability because discrepancies among measured amounts greatly exceed the estimated errors induced by different measurement methods (Hansen et al., 2004).

3 Model description

The model GISS-PUCCINI is the NASA Goddard Institute for Space Studies (GISS) atmospheric composition and climate model. It consists of the model for Physical Understanding of Composition-Climate Interactions and Impacts (PUCCINI) (Shindell et al., 2006), which is fully embedded in the GISS modelE climate model (Schmidt et al., 2006). The atmospheric model version used here, GISS-E2, is that used for the Coupled Model Intercomparison Project (CMIP) phase 5 simulations in support of the IPCC

ACPD
12, 11245–11274, 2012

fifth assessment report (AR5), and contains updates to the physics relevant to aerosols, including the ability to represent multiple downdrafts and updrafts in convective systems, while the black carbon model is unchanged from Koch and Hansen (2005). The model was run at 2° latitude by 2.5° longitude horizontal resolution with 40 vertical layers. Simulations were performed for 1995–2009 using observed sea surface temperatures (Rayner et al., 2003) and linear relaxation of winds toward either NCEP or MERRA reanalysis (Kalnay et al., 1996; Rienecker et al., 2011), with results analyzed for 2006–2009. Repeating year 2000 monthly-varying emissions were used from the data set assembled for the AR5 simulations (Lamarque et al., 2010) with the exception of biomass burning emissions which were monthly- and annually-varying emissions from the Global Fire Emission Database (GFED) version 3 (van der Werf et al., 2010).

4 Initial field in the Arctic Ocean

Another issue that needs to be considered is the initial snow cover (depth and density) and sBC distribution over multiyear sea ice at the beginning of the accumulation and deposition season (in this study: September). The initial field represents the snow and BC content within it that survived melt season. Because thermodynamic and dynamic models of sea ice cover are limited in their ability to simulate the time-varying ice conditions during the summer, we assume the initial snow cover to be that of the September climatological snow conditions in Warren et al. (1999), which was also applied in the estimation of snow depth in (Kwok et al., 2008). The observations of snow and ice density (recent snow: $0.102 \pm 0.019\,\mathrm{g\,cm^{-3}}$, surface ($< 3\,\mathrm{cm}$): $0.291 \pm 0.056\,\mathrm{g\,cm^{-3}}$, subsurface ($> 3\,\mathrm{m}$): $0.333 \pm 0.02\,\mathrm{g\,cm^{-3}}$) in the 3th Chinese Arctic expedition route (79.8–85.4° N, 144.1–170.1° W) in summer 2008 have been applied in the estimation of snow water equivalent (SWE) and in the calculation of vertically-integrated concentrations of sBC from surface and subsurface measurements. In our construction, we maintain a separate record of the initial conditions (sBC, SWE and density) at each grid point. Table 2 summarizes the original observations and estimated values of sBC in the Arctic Ocean

ACPD
12, 11245–11274, 2012

in summer 2005, 2008 and 2010. These measurements range from 74° N to 89° N, all of them are used to represent the climatological distribution of sBC over the multiyear sea ice in summer. The entire Arctic Ocean is divided into three latitudinal bands: south of 80° N, 80–85° N and the Arctic Ocean center, the distribution of sBC in each band is represented by the mean values of the observations located within it. In this case, the initial fields are not time-varying and are identical for the results shown in this work.

5 Intercomparison between model results and observations

Present observations of sBC show sketchy but identifiable variation in spatial distribution, with maximum values in the Russian Arctic and much lower values in other regions. From the simulations calculated from the model dry and wet deposition in spring 2007–2009, we can see that model values are also higher over the Eurasian than the Canadian and Alaskan Arctic, followed by the Arctic Ocean, with the lowest in Greenland (Fig. 3). There is an apparent gradient from around the coast to the Central Arctic Ocean, especially in the Russian Arctic but relatively little variability over the Arctic Ocean. The mean concentration of sBC over the Arctic Ocean shows large interannual variability in spring from 2007 to 2009 (7.8–13.4 $ng\,g^{-1}$). Point to point comparisons between measured sBC and model simulations from NCEP run and MERRA runs have been carried out respectively in the Arctic Ocean and surrounding seas, the Canadian and Alaskan Arctic, the Russian Arctic, Svalbard and Greenland (Fig. 4). Model results have been interpolated to each measurement site in the corresponding month and year of observations and are compared with the mean observed value in cases where more than one measurement is available within a 2° × 2.5° grid box. From Fig. 4a, it can be seen that the values of modeled sBC are comparable with present observations over each Arctic region despite a certain degree of underestimation. The correlation coefficient between them can be up to 0.64 (for NCEP run in Fig. 4b and 0.6 for MERRA run). That said, the model result from NCEP run is closer to the measured sBC than that from the MERRA run. Hence we recommend the NCEP reanalyses are a better choice for

ACPD
12, 11245–11274, 2012

current GISS simulation of BC in the Arctic. The ratio of observed to modeled sBC is 1.1. Rough agreement between the model and observations is found in the Canadian Arctic sector, with mean values of $7.2 \pm 1.3\,ng\,g^{-1}$ in the model and $7.8 \pm 2.4\,ng\,g^{-1}$ in the observations. The concentrations of modeled sBC in Western Greenland in spring 2008 are also close to the observations; mean values are $3.8 \pm 1.8\,ng\,g^{-1}$ in the model and $3.8 \pm 0.7\,ng\,g^{-1}$ in the observations. However, there is an apparent difference in Northern Greenland, that conform to the abnormal high-value center in the inland areas of Greenland (Fig. 3), more measurements would be needed to know the actual distribution of sBC here. Similar situation occurred in the center regions of the Arctic Ocean, from the bottom left panel in Fig. 3, it can be seen that the simulated high value zone was generally located in the north of Canada Basin and in the center of the Arctic Ocean. Most observations in these areas are from the surface snow rather than the whole layer of snow, which would be the main reason for the bias in the Arctic Ocean. Additionally, the values of modeled sBC are significantly smaller than observations in the Russian Arctic sector in spring 2007. Previous studies indicate that anthropogenic influence was dominant in Western Russia in spring 2007, and open fire influence was dominant in Eastern Russia in spring 2008 (Doherty et al., 2010; Wang et al., 2011). Indeed, values in Eastern Russia are substantially higher in the model in 2008 than in 2007, perhaps owing to the interannually varying biomass burning emissions. Hence an underestimation of biomass burning emissions in Russia may be the main reason of this simulation bias.

The simulation values in Svalbard are within the range of observations and near to the median value. Analysis of previous measurements (81 samples) in Svalbard indicates that there exist obvious spatial variations, the concentrations of sBC in Eastern Svalbard are significantly higher than the western side (Forsstrom et al., 2009) and the emissions from the Western European Arctic may be dominant in this distribution pattern. This spatial variation has also been reproduced by the model even though the modeled concentrations in Western Svalbard are a little higher than the observed concentrations.

ACPD
12, 11245–11274, 2012

We also estimate the decrease in snow and sea ice albedo and resulting radiative forcing based on the sBC distribution simulated by the current GISS-PUCCINI model. Figure 5 shows the albedo decreases in and around the Arctic Ocean in spring 2007–2009 due to BC deposition. We estimate the impact of sBC on snow and ice albedo according to the Fig. 2 in Warren and Wiscombe (1985) and assume the snow grain radius is a constant of 100 µm (McConnell et al., 2007) with no significant aging. The calculated decrease in snow and ice albedo averaged in and around the Arctic Ocean (66–90° N) is 0.4–0.6 % from spring 2007–2009, lower than the estimates of Park et al. (2005), but comparable with Jacobson et al. (2004). On the basis of this result of albedo decrease, we evaluate the radiative forcing caused by sBC with the NCEP downwelling surface solar radiation. Result shows that the radiative forcings from BC deposition to the Arctic snow and ice (north to 66° N) are 0.7 $W m^{-2}$, 1.1 $W m^{-2}$ and 1.0 $W m^{-2}$, respectively in spring 2007, 2008 and 2009. Wang et al. (2011) reported a radiative forcing of 1.2 $W m^{-2}$ for spring 2007–2009 in the Arctic north to 60° N, similar to Flanner et al. (2007) and slightly larger than our values. This discrepancy may result from different domain used in the analysis, and the underestimation of sBC in the Russian Arctic may be another reason.

Finally, we review the research on the potential source type/region of Arctic BC in previous studies. Rahn et al. (1980) first indicates that the Arctic atmosphere is hazy in winter and spring, that resulting from fossil fuel burning, industrial, and agricultural processes, by long-range transport of mid-latitude pollution products. Generally, Europe, North America and South Asia are considered to be the main contributors to present Arctic sBC, and biomass sources are dominant (Hegg et al., 2009). Matsui et al. (2011) suggests that biomass burning and anthropogenic sources in high-latitude were most important for the Arctic BC both in spring and summer, because most of BC from lower-latitude regions has been removed by wet deposition before arriving at the Arctic. Among these source regions, Europe contributes more than 50 % of the Arctic BC loading mainly through transport within the lower troposphere in all seasons (Huang et al., 2010b), which is the most likely cause of the highest concentrations in

ACPD
12, 11245–11274, 2012

the Russian Arctic and surrounding Seas. Hegg et al. (2009) also indicates that local emissions from fossil-fuel combustion make a significant contribution to the springtime high-latitude Arctic Ocean and some locations in Western Russia. North America contributes about 10–20 % to the Arctic troposphere with least variations in the contribution from different vertical levels (Huang et al., 2010b; Shindell et al., 2008), and is also regarded as a main biomass source to Greenland, the Alaskan and the Canadian Arctic (McConnell et al., 2007; Hegg et al., 2009). Because of its remoteness from the main source regions, the concentrations in Greenland and the Central Arctic Ocean are much lower than other Arctic regions. South Asia is also considered to be a significant contributor in the Arctic upper troposphere/lower stratosphere during the springtime but it does not appear to contribute significantly to the deposited BC (Koch and Hansen, 2005; Hirdman et al., 2010). In addition to the pollution from long range transport sources, the emissions from ships and cross-polar aircraft flight are also very important. Corbett et al. (2007) indicates that the impacts from local shipping are comparable with long range transport from lower latitude emission sources. Emission form international shipping can be up to 71 000–160 000 metric tons annually, representing about 2 % of global BC from all sources. It is also shown that 1.2 Gg BC has been emitted from shipping within the Arctic in 2004, most of which was derived from transit vessels, container and general cargo ships, and the rest from fishing vessels (Corbett et al., 2010a). The vessel activities are mainly concentrated in summer and autumn months, and are increasing dramatically with the rapid decrease of the Arctic sea ice. In this background, many approaches have been recommended to reduce PM emissions from diesel engines and ships, such as switching to low-sulfur fuels and engine process modifications (Corbett et al., 2010b). Cross-polar aircraft flight is also an important contributor to the Arctic BC. Whitt et al. (2011) point out that 2.35 Tg fuel were burned in the Arctic Circle (66.56° N–90° N) in 2006 and more than half of commercial aviation emissions occur in relatively stable regions of the atmosphere and nearly one quarter occur in the stratosphere. In view of the validation against present spatially

ACPD
12, 11245–11274, 2012

extensive observations of sBC, we suggest that the latest NASA GISS-E2-PUCCINI model would be a rational choice to further identify source regions of Arctic BC.

6 Discussion and conclusions

There are large uncertainties in current model simulations of BC in the Arctic. Various models give very different regional source contributions and different evaluation of radiative forcing due to BC deposition. It is useful to characterize model biases by comparing results with present field observations, in order to reduce these uncertainties. In this study, spatially extensive comparisons between model results and present sBC observations are carried out, to validate the latest GISS model deposition of BC in the Arctic regions. It is demonstrated that the latest GISS model performs well in large scale simulations of BC deposition, especially in the Canadian Arctic sector. The overall ratio of observed to modeled sBC is 1.1. This suggests that there is underestimation to some extent in current simulation of sBC (which also can be seen from Fig. 4a). Further comparison of modeled aBC with surface long-term observations in Barrow, Alert, Zeppelin and Nord stations shows that the latest GISS model has been greatly improved in simulating the seasonal variations of the Arctic BC (Fig. 6), in comparison to previous edition mentioned in Shindell et al. (2008), but still has significant underestimation in winter and spring, especially at Barrow station, where the bias can be up to one order of magnitude. This is in agreement with the results of Koch et al. (2009b), in which they indicated that GISS model could reproduce a rough shape of observed vertical profiles in North of Greenland, Canadian and North American Arctic in spring period, but with underestimation throughout much of the troposphere, especially in Alaskan Arctic regions. From these, we can conclude that current GISS model give a general underestimation of BC in the Arctic troposphere layer during the measurement period. Taking into account that BC in Arctic snow and ice mainly originates from dry deposition from the lowest atmosphere as well as scavenging from lower or higher levels in the atmosphere (Quinn et al., 2011), we suggest that current underestimation of aBC

ACPD
12, 11245–11274, 2012

in troposphere layer may be the main reason for the underestimation of BC deposition to Arctic snow and sea ice.

It is especially worth noting that the largest simulation biases appear in the Russian Arctic (see Fig. 4, upper panel). Though there are few measurement points included in the comparison in this region, we expect that biomass burning emissions may be the main cause of the poor performance here, though Arctic industrial emissions could also play a role. There are two pieces of evidence to support this opinion, (1) biomass burning and anthropogenic sources in high-latitude were regarded as the most important contributor to the Arctic BC (Matsui et al., 2011), and emission from biomass burning is dominant in the contribution to Arctic sBC (Hegg et al., 2009). (2) Strong cooling of the air over the snow cover in Eurasia allows polluted air from Northern Eurasia to penetrate the entire Arctic at low altitudes (Stohl et al., 2006) and Northern Eurasia is most likely to be the source region of the aBC in the lower troposphere in the Arctic in winter and early spring (Quinn et al., 2011). It is still not enough to make a conclusion just according to the above analyses. Further model simulations of BC are needed to determine if emissions are responsible, and if so to show which emissions from what regions and which type of sources lead to the current bias in the Russian Arctic. For example, running the model in a period when Russian forest fires were minimal. In addition to the inherent problems in the model, the approximations and hypotheses used in the calculation of vertically-integrated concentration of sBC may be another reason for the underestimation. We applied climatological observations of snow density obtained in the SHEBA campaign to stand for the actual values of snow density in different depths at each measurement site, this may lead to much larger uncertainties in the Russian Arctic than other Arctic regions, as significant variations in the vertical profiles are observed there. More measurements of snow density in various snow depths are needed to reduce this uncertainty. It also needs to be validated whether the SHEBA observations can represent the distribution of snow density in other Arctic regions.

ACPD
12, 11245–11274, 2012

Acknowledgements. We especially thank S. J. Doherty who supplied most of the snow black carbon observations and gave valuable comments on this study. We would like to thank the anonymous referee for their valuable comments greatly improving the paper. We also would like to thank Chinese Arctic and Antarctic Administration for providing the opportunities of participating in the two Arctic expeditions and the kindly help of all staff in the 3rd Chinese Arctic expedition and the 1st Korean Arctic expedition. The concentrations of black carbon are measured in Center for Atmosphere Watch and Service, Chinese Academy of Meteorological Sciences. This work was funded by the Opening Founding of State Key Laboratory of Cryospheric Sciences (SKLCS 09-07) and National Basic Research Program of China (2011CB403401, 2010CB955608).

References

Clarke, A. and Noone, K.: Soot in the Arctic: a cause for perturbation in radiative transfer, J. Geophys. Res., 19, 2045–2053, 1985.

Chylek, P., Srivastava, V., Cahenzli, L., Pinnick, R. G., Dod, R. L., and Novakov, T.: Aerosol and graphitic carbon content of snow, J. Geophys. Res., 92, 9801–9809, 1987.

Cachier, H.: Particulate and dissolved carbon in air and snow at the Summit site, in: Transfer of Aerosols and Gases to Greenland Snow and Ice: Final Technical Report, Cedex, France, 21–27, 1997.

Corbett, J. J., Wang, C., Winebrake, J. J., and Green, E.: Review of Marpol Annex VI and the NO_x Technical Code: Allocation and Forecasting of Global Ship Emissions, International Maritime Organization, London, UK, 27 pp., 2007.

Corbett, J. J., Lack, D. A., Winebrake, J. J., Harder, S., Silberman, J. A., and Gold, M.: Arctic shipping emissions inventories and future scenarios, Atmos. Chem. Phys., 10, 9689–9704, doi:10.5194/acp-10-9689-2010, 2010a.

Corbett, J. J., Winebrake, J., and Green, E.: An assessment of technologies for reducing regional short-lived climate forcers emitted by ships with implications for Arctic shipping, Carbon Manage., 1, 207–225, 2010b.

Doherty, S. J., Warren, S. G., Grenfell, T. C., Clarke, A. D., and Brandt, R. E.: Light-absorbing impurities in Arctic snow, Atmos. Chem. Phys., 10, 11647–11680, doi:10.5194/acp-10-11647-2010, 2010.

ACPD

12, 11245–11274, 2012

Flanner, M. G., Zender, C. S., Randerson, J. T., and Rasch, P. J.: Present-day climate forcing and response from black carbon in snow, J. Geophys. Res., 112, D11202, doi:10.1029/2006JD008003, 2007.

Forsstrom, S., Strom, J., Pedersen, C. A., Isaksson, E., and Gerland, S.: Elemental carbon distribution in Svalbard snow, J. Geophys. Res., 114, D19112, doi:10.1029/2008JD011480, 2009.

Grenfell, T., Light, B., and Sturm, M.: Spatial distribution and radiative effects of soot in the snow and sea ice during the SHEBA experiment, J. Geophys. Res., 107, 8032, doi:10.1029/2000JC000414, 2002.

Hansen, J. and Nazarenko, L.: Soot climate forcing via snow and ice albedos, Proc. Natl. Acad. Sci., 101, 423–428, doi:10.1073/pnas.2237157100, 2004.

Hansen, J., Sato, M., Ruedy, R., Kharecha, P., Lacis, A., Miller, R. L., Nazarenko, L., Lo, K., Schmidt, G. A., Russell, G., Aleinov, I., Bauer, S., Baum, E., Cairns, B., Canuto, V., Chandler, M., Cheng, Y., Cohen, A., Del Genio, A., Faluvegi, G., Fleming, E., Friend, A., Hall, T., Jackman, C., Jonas, J., Kelley, M., Kiang, N. Y., Koch, D., Labow, G., Lerner, J., Menon, S., Novakov, T., Oinas, V., Perlwitz, J. P., Perlwitz, Ju., Rind, D., Romanou, A., Schmunk, R., Shindell, D., Stone, P., Sun, S., Streets, D., Tausnev, N., Thresher, D., Unger, N., Yao, M., and Zhang, S.: : Climate simulations for 1880–2003 with GISS modelE, Clim. Dynam., 29, 661–696, doi:10.1007/s00382-007-0255-8, 2007.

Hegg, D. A., Warren, S. G., Grenfell, T. C., Doherty, S. J., Larson, T. V., and Clarke, A. D.: Source attribution of black carbon in Arctic snow, Environ. Sci. Technol., 43, 4016–4021, 2009.

Hirdman, D., Sodemann, H., Eckhardt, S., Burkhart, J. F., Jefferson, A., Mefford, T., Quinn, P. K., Sharma, S., Ström, J., and Stohl, A.: Source identification of short-lived air pollutants in the Arctic using statistical analysis of measurement data and particle dispersion model output, Atmos. Chem. Phys., 10, 669–693, doi:10.5194/acp-10-669-2010, 2010.

Huang, L., Gong, S. L., Jia, C. Q., and Lavoue, D.: Importance of deposition process in simulating the seasonality of the Arctic black carbon aerosol, J. Geophys. Res., 115, D17207, doi:10.1029/2009JD013478, 2010a.

Huang, L., Gong, S. L., Jia, C. Q., and Lavoue, D.: Relative contributions of anthropogenic emissions to black carbon aerosol in the Arctic, J. Geophys. Res., 115, D19208, doi:10.1029/2009JD013592, 2010b.

Intergovernmental Panel on Climate Change: IPCC Fourth Assessment Report, Climate Change 2007: The Scientific Basis, Cambridge University Press, New York, 2007.

ACPD
12, 11245–11274, 2012

Jacobson M. Z.: Strong radiative heating due to the mixing state of black carbon in atmospheric aerosols, Nature, 409, 695–697 doi:10.1038/35055518, 2001.

Jacobson, M. Z.: The climate response of fossil-fuel and biofuel soot, accounting for soot's feedback to snow and sea ice albedo and emissivity, J. Geophys. Res., 109, D21201, doi:10.1029/2004JD004945, 2004.

Kalnay, E., Kanamitsu, M., Kistler, R., Collins, W., Deaven, D., Gandin, L., Iredell, M., Saha, S., White, G., Woollen, J., Zhu, Y., Leetmaa, A., Reynolds, R., Chelliah, M., Ebisuzaki, W., Higgins, W., Janowiak, J., Mo, K. C., Ropelewski, C., Wang, J., Jenne, R., and Joseph, D.: The NCEP/NCAR 40-year reanalysis project, Bull. Am. Meteorol. Soc., 77, 437–471, 1996.

Koch, D. and Hansen, J.: Distant origins of Arctic black carbon: a goddard institute for space studies modelE experiment, J. Geophys. Res., 110, D04204, doi:10.1029/2004JD005296, 2005.

Koch, D., Menon, S., Del Genio, A., Ruedy, R., Aleinov, I., and Schmidt, G. A.: Distinguishing aerosol impacts on climate over the past century, J. Climate, 22, 2659–2677, 2009a.

Koch, D., Schulz, M., Kinne, S., McNaughton, C., Spackman, J. R., Balkanski, Y., Bauer, S., Berntsen, T., Bond, T. C., Boucher, O., Chin, M., Clarke, A., De Luca, N., Dentener, F., Diehl, T., Dubovik, O., Easter, R., Fahey, D. W., Feichter, J., Fillmore, D., Freitag, S., Ghan, S., Ginoux, P., Gong, S., Horowitz, L., Iversen, T., Kirkevåring, A., Klimont, Z., Kondo, Y., Krol, M., Liu, X., Miller, R., Montanaro, V., Moteki, N., Myhre, G., Penner, J. E., Perlwitz, J., Pitari, G., Reddy, S., Sahu, L., Sakamoto, H., Schuster, G., Schwarz, J. P., Seland, Ø., Stier, P., Takegawa, N., Takemura, T., Textor, C., van Aardenne, J. A., and Zhao, Y.: Evaluation of black carbon estimations in global aerosol models, Atmos. Chem. Phys., 9, 9001–9026, doi:10.5194/acp-9-9001-2009, 2009b.

Kwok, R. and Cunningham, G. F.: ICESat over Arctic sea ice: estimation of snow depth and ice thickness, J. Geophys. Res., 113, C08010, doi:10.1029/2008JC004753, 2008.

Lamarque, J.-F., Bond, T. C., Eyring, V., Granier, C., Heil, A., Klimont, Z., Lee, D., Liousse, C., Mieville, A., Owen, B., Schultz, M. G., Shindell, D., Smith, S. J., Stehfest, E., Van Aardenne, J., Cooper, O. R., Kainuma, M., Mahowald, N., McConnell, J. R., Naik, V., Riahi, K., and van Vuuren, D. P.: Historical (1850–2000) gridded anthropogenic and biomass burning emissions of reactive gases and aerosols: methodology and application, Atmos. Chem. Phys., 10, 7017–7039, doi:10.5194/acp-10-7017-2010, 2010.

ACPD
12, 11245–11274, 2012

Liu, J. Fan, S., Horowitz, L. W., and Levy, H.: II February: evaluation of factors controlling long-range transport of black carbon to the Arctic, J. Geophys. Res., 116, D04307, doi:10.1029/2010JD015145, 2011.

Matsui, H., Kondo, Y., Moteki, N., Takegawa, N., Sahu, L. K., Zhao, Y., Fuelberg, H. E., Sessions, W. R., Diskin, G., Blake, D. R., Wisthaler, A., and Koike, M.: Seasonal variation of the transport of black carbon aerosol from the Asian continent to the Arctic during the ARCTAS aircraft campaign, J. Geophys. Res., 116, D05202, doi:10.1029/2010JD015067, 2011.

McConnell, J. R., Edwards, R., Kok, G. L., Flanner, M. G., Zender, C. S., Saltzman, E. S., Banta, J. R., Pasteris, D. R., Carter, M. M., and Kahl, J. D. W.: 20th-century industrial black carbon emissions altered Arctic climate forcing, Science, 317, 1381–1384, doi:10.1126/science.1144856, 2007.

Ming, J., Cachier, H., Xiao, C., Qin, D., Kang, S., Hou, S., and Xu, J.: Black carbon record based on a shallow Himalayan ice core and its climatic implications, Atmos. Chem. Phys., 8, 1343–1352, doi:10.5194/acp-8-1343-2008, 2008.

Park, R. J., Jacob, D. J., Palmer, P. I., Clarke, A. D., Weber, R. J., Zondlo, M. A., Eisele, F. L., Bandy, A. R., Thornton, D. C., Sachse, G. W., and Bond, T. C.: Export efficiency of black carbon aerosol in continental outflow: global implications, J. Geophys. Res.-Atmos., 110, D11205, doi:10.1029/2004JD005432, 2005.

Quinn, P. K., Bates, T. S., Baum, E., Doubleday, N., Fiore, A. M., Flanner, M., Fridlind, A., Garrett, T. J., Koch, D., Menon, S., Shindell, D., Stohl, A., and Warren, S. G.: Short-lived pollutants in the Arctic: their climate impact and possible mitigation strategies, Atmos. Chem. Phys., 8, 1723–1735, doi:10.5194/acp-8-1723-2008, 2008.

Quinn, P. K., Stohl, A., Arneth, A., Berntsen, T., Burkhart, J. F., Christensen, J., Flanner, M., Kupiainen, K., Lihavainen, H., Shepherd, M., Shevchenko, V., Skov, H., and Vestreng, V.: The impact of black carbon on Arctic climate, Arctic Monitoring and Assessment Programme (AMAP), Oslo, 72 pp., 2011.

Rahn, K. A. and McCaffrey, R. J.: On the origin and transport of the winter arctic aerosol, Ann. NY Acad. Sci., 338, 486–503, 1980.

Rayner, N. A., Parker, D. E., Horton, E. B., Folland, C. K., Alexander, L. V., Rowell, D. P., Kent, E. C., and Kaplan, A.: Global analyses of sea surface temperature, sea ice, and night marine air temperature since the late nineteenth century, J. Geophys. Res., 108, 4407, doi:10.1029/2002JD002670, 2003.

ACPD
12, 11245–11274, 2012

Rienecker, M. M., Suarez, M. J., Gelaro, R., Todling, R., Bacmeister, J., Liu, E., Bosilovich, M. G., Schubert, S. D., Takacs, L., Kim, G., Bloom, S., Chen, J., Collins, D., Conaty, A., Silva, A. D., Gu, W., Joiner, J., Koster, R. D., Lucchesi, R., Molod, A., Owens, T., Pawson, S., Pegion, P., Redder, C. R., Reichle, R., Robertson, F. R., Ruddick, A. G., Sienkiewicz, M., and Woollen, J.: MERRA: NASA's Modern-Era Retrospective Analysis for Research and Applications, J. Climate, 24, 3624–3648, 2011.

Schmidt, G. A., Ruedy, R., Hansen, J. E., Aleinov, I., Bell, N., Bauer, M., Bauer, S., Cairns, B., Canuto, V., Cheng, Y., Genio, A. D., Faluvegi, G., Friend, A. D., Hall, T. M., Hu, Y., Kelley, M., Kiang, N. Y., Koch, D., Lacis, A. A., Lerner, J., Lo, K. K., Miller, R. L., Nazarenko, L., Oinas, V., Perlwitz, J., Perlwitz, J., Rind, D., Romanou, A., Russell, G. L., Sato, M., Shindell, D. T., Stone, P. H., Sun, S., Tausney, N., Thresher, D., and Yao, M.: Present-day atmospheric simulations using GISS ModelE: comparison to in situ, satellite, and reanalysis data, J. Climate, 19, 153–192, 2006.

Shindell, D. T., Faluvegi, G., Unger, N., Aguilar, E., Schmidt, G. A., Koch, D. M., Bauer, S. E., and Miller, R. L.: Simulations of preindustrial, present-day, and 2100 conditions in the NASA GISS composition and climate model G-PUCCINI, Atmos. Chem. Phys., 6, 4427–4459, doi:10.5194/acp-6-4427-2006, 2006.

Shindell, D. T., Chin, M., Dentener, F., Doherty, R. M., Faluvegi, G., Fiore, A. M., Hess, P., Koch, D. M., MacKenzie, I. A., Sanderson, M. G., Schultz, M. G., Schulz, M., Stevenson, D. S., Teich, H., Textor, C., Wild, O., Bergmann, D. J., Bey, I., Bian, H., Cuvelier, C., Duncan, B. N., Folberth, G., Horowitz, L. W., Jonson, J., Kaminski, J. W., Marmer, E., Park, R., Pringle, K. J., Schroeder, S., Szopa, S., Takemura, T., Zeng, G., Keating, T. J., and Zuber, A.: A multi-model assessment of pollution transport to the Arctic, Atmos. Chem. Phys., 8, 5353–5372, doi:10.5194/acp-8-5353-2008, 2008.

Slater, J. F., Currie, L. A., Dibb, J. E., and Benner, J. B. A.: Distinguishing the relative contribution of fossil fuel and biomass combustion aerosols deposited at Summit, Greenland through isotopic and molecular characterization of insoluble carbon, Atmos. Environ., 36, 4463–4477, 2002.

Stohl, A.: Characteristics of atmospheric transport into the arctic troposphere, J. Geophys. Res., 111, D11306, doi:10.1029/2005JD006888, 2006.

Sturm, M., Holmgren, J., and Perovich, D. K.: Winter snow cover on the sea ice of the Arctic Ocean at the Surface Heat Budget of the Arctic Ocean (SHEBA): temporal evolution and spatial variability, J. Geophys. Res., 107, 8047, doi:10.1029/2000JC000400, 2002.

ACPD
12, 11245–11274, 2012

van der Werf, G. R., Randerson, J. T., Giglio, L., Collatz, G. J., Mu, M., Kasibhatla, P. S., Morton, D. C., DeFries, R. S., Jin, Y., and van Leeuwen, T. T.: Global fire emissions and the contribution of deforestation, savanna, forest, agricultural, and peat fires (1997–2009), Atmos. Chem. Phys., 10, 11707–11735, doi:10.5194/acp-10-11707-2010, 2010.

Wang, Q., Jacob, D. J., Fisher, J. A., Mao, J., Leibensperger, E. M., Carouge, C. C., Le Sager, P., Kondo, Y., Jimenez, J. L., Cubison, M. J., and Doherty, S. J.: Sources of carbonaceous aerosols and deposited black carbon in the Arctic in winter-spring: implications for radiative forcing, Atmos. Chem. Phys., 11, 12453–12473, doi:10.5194/acp-11-12453-2011, 2011.

Warren, S. G. and Wiscombe, W. J.: Dirty snow after nuclear war, Nature, 313, 467–470, 1985.

Warren, S. G., Rigor, I. G., and Untersteiner, N.: Snow depth on Arctic sea ice, J. Climate, 12, 1814–1829, 1998.

Whitt, D. B., Wilkerson, J. T., Jacobson, M. Z., Naiman, A. D., and Lele, S. K.: Vertical mixing of commercial aviation emissions from cruise altitude to the surface, J. Geophys. Res., 116, D14109, doi:10.1029/2010JD015532, 2011.

ACPD
12, 11245–11274, 2012

Table 1. Present-day sBC observations in and around the Arctic Ocean in spring. The estimated sBC in this study are calculated from surface and subsurface concentrations with the snow densities obtained in SHEBA field campaign. Most of the surface and subsurface values listed in this table are from Doherty et al. (2010) and others are from several field campaigns known to us. The measurements within a single model grid ("8–12", "28–29", "40–41", "42–45", "49–59", "60–66", "67–69") are averaged before the comparison with modeled sBC.

NO.	Measurement Region	Lat (° N)	Lon (° E)	Surface	Subsurface	Whole layer	Measurement period	Reference	Estimated sBC (ngg^{-1})	Uncertainty of Estimation
1	Arctic Ocean	82.880	205.550	–	–	7.00	Apr–May, 2006	NPEO (Field compaign)	7.00	–
2	Arctic Ocean	84.700	296.520	–	–	5.00	Apr–May, 2008	Switchyard campaign	5.00	–
3	Arctic Ocean	86.300	334.830	–	–	6.75	Apr–May, 2008	Switchyard campaign	6.75	–
4	Arctic Ocean	88.100	269.280	–	–	6.26	Spring, 2008	Doherty et al. [2010)	6.26	–
5	Arctic Ocean	88.560	314.375	–	–	5.00	Apr–May, 2008	Switchyard campaign	5.00	–
6	Arctic Ocean	89.700	336.400	–	–	3.00	Apr–May, 2007	NPEO (Field compaign)	3.00	–
7	N. Pole	89.200	257.500	–	–	3.81	Spring, 2008	Doherty et al. (2010)	3.81	–
8	N. Pole	89.300	358.120	–	–	4.85	Spring, 2008	Doherty et al. (2010)	4.85	–
9	N. Pole	89.400	359.000	–	–	2.33	Spring, 2008	Doherty et al. (2010)	2.33	–
10	N. Pole	89.500	358.930	–	–	2.51	Spring, 2008	Doherty et al. (2010)	2.51	–
11	N. Pole	89.900	329.400	–	–	4.20	Spring, 2008	Doherty et al. (2010)	4.20	–
12	N. Pole	90.000	0.980	–	–	4.00	Spring, 2008	Doherty et al. (2010)	4.00	–
13	Beaufort Sea	73.000	215.000	9.94	8.63	–	Apr, 2007	APLIS/SEDNA campaign	8.89	0.08
14	Beaufort Sea	74.020	214.610	–	–	12.00	Apr, 2007	APLIS/SEDNA campaign	12.00	–
15	Beaufort Sea	75.340	224.343	–	–	11.46	Apr, 2007	APLIS/SEDNA campaign	11.46	–
16	Beaufort Sea	79.540	203.110	–	–	8.00	Apr, 2007	APLIS/SEDNA campaign	8.00	–
17	Canadian Arctic	66.171	255.626	13.90	6.68	–	Spring, 2009	Doherty et al. (2010)	8.11	0.46
18	Canadian Arctic	67.878	283.530	9.40	4.20	–	Spring, 2009	Doherty et al. (2010)	5.23	0.33
19	Canadian Arctic	68.305	255.913	6.97	10.30	–	Spring, 2009	Doherty et al. (2010)	9.64	0.21
20	Canadian Arctic	68.568	230.477	9.10	6.57	–	Spring, 2009	Doherty et al. (2010)	7.07	0.16
21	Canadian Arctic	68.824	264.711	12.40	7.30	–	Spring, 2009	Doherty et al. (2010)	8.31	0.32
22	Canadian Arctic	68.986	224.938	7.15	11.55	–	Spring, 2009	Doherty et al. (2010)	10.68	0.28
23	Canadian Arctic	69.280	282.954	8.60	5.13	–	Spring, 2009	Doherty et al. (2010)	5.82	0.22
24	Alaskan Arctic	69.300	216.200	5.00	–	–	Spring, 2009	Doherty et al. (2010)	5.00	–
25	Canadian Arctic	69.635	227.819	10.00	9.00	–	Spring, 2009	Doherty et al. (2010)	9.20	0.06
26	Canadian Arctic	69.663	250.904	7.10	5.70	–	Spring, 2009	Doherty et al. (2010)	5.98	0.09
27	Canadian Arctic	69.895	247.253	6.00	13.87	–	Spring, 2009	Doherty et al. (2010)	12.31	0.50
28	Canadian Arctic	70.067	235.027	15.90	10.50	–	Spring, 2009	Doherty et al. (2010)	11.57	0.34
29	Canadian Arctic	70.067	235.027	12.10	5.30	–	Spring, 2009	Doherty et al. (2010)	6.65	0.43
30	Canadian Arctic	71.151	280.752	4.70	3.43	–	Spring, 2009	Doherty et al. (2010)	3.68	0.08
31	Alaskan Arctic	71.325	203.567	9.00	–	–	Spring, 2009	Doherty et al. (2010)	9.00	–
32	Canadian Arctic	72.341	277.645	9.50	3.24	–	Spring, 2009	Doherty et al. (2010)	4.48	0.40
33	Canadian Arctic	72.566	259.193	15.20	6.30	–	Spring, 2009	Doherty et al. (2010)	8.06	0.57
34	Canadian Arctic	75.497	263.855	9.97	9.40	–	Spring, 2009	Doherty et al. (2010)	9.51	0.04
35	Canadian Arctic	76.555	255.268	9.32	8.65	–	Spring, 2009	Doherty et al. (2010)	8.78	0.04
36	Canadian Arctic	76.633	263.788	11.70	3.80	–	Spring, 2009	Doherty et al. (2010)	5.37	0.50
37	Canadian Arctic	76.867	274.786	9.20	5.83	–	Spring, 2009	Doherty et al. (2010)	6.50	0.21
38	Canadian Arctic	80.083	273.300	12.00	–	–	Spring, 2007	Doherty et al. (2010)	12.00	–
39	Western Russia	67.631	53.646	19.00	8.00	–	Spring, 2007	Doherty et al. (2010)	10.18	0.70
40	Western Russia	73.381	81.429	17.60	21.65	–	Spring, 2007	Doherty et al. (2010)	20.85	0.26

ACPD
12, 11245–11274, 2012

Table 1. Continued.

NO.	Measurement Region	Lat (°N)	Lon (°E)	Surface	Subsurface	Whole layer	Measurement period	Reference	Estimated sBC ($ng\,g^{-1}$)	Uncertainty of Estimation
41	Western Russia	73.428	81.481	12.00	27.00	–	Spring, 2007	Doherty et al. (2010)	24.03	0.95
42	Western Russia	72.176	102.839	83.60	34.20	–	Spring, 2007	Doherty et al. (2010)	44.00	3.14
43	Western Russia	72.211	102.933	23.20	27.90	–	Spring, 2007	Doherty et al. (2010)	26.97	0.30
44	Western Russia	72.277	103.102	45.80	40.40	–	Spring, 2007	Doherty et al. (2010)	41.47	0.34
45	Western Russia	72.244	103.019	62.10	40.90	–	Spring, 2007	Doherty et al. (2010)	45.10	1.35
46	Eastern Russia	72.054	128.523	87.90	17.60	–	Spring, 2008	Doherty et al. (2010)	31.54	4.47
47	Eastern Russia	74.065	128.872	13.00	26.00	–	Spring, 2008	Doherty et al. (2010)	23.42	0.83
48	Eastern Russia	71.649	127.894	82.00	25.80	–	Spring, 2008	Doherty et al. (2010)	36.94	3.57
49	Eastern Russia	68.631	160.369	83.20	15.50	–	Spring, 2008	Doherty et al. (2010)	28.92	4.30
50	Eastern Russia	68.649	160.487	80.00	14.00	–	Spring, 2008	Doherty et al. (2010)	27.09	4.20
51	Eastern Russia	68.663	160.592	88.30	18.50	–	Spring, 2008	Doherty et al. (2010)	32.34	4.44
52	Eastern Russia	69.043	161.122	55.60	23.50	–	Spring, 2008	Doherty et al. (2010)	29.87	2.04
53	Eastern Russia	69.044	161.123	53.15	19.90	–	Spring, 2008	Doherty et al. (2010)	26.49	2.11
54	Eastern Russia	69.032	161.201	50.00	26.00	–	Spring, 2008	Doherty et al. (2010)	30.76	1.53
55	Eastern Russia	69.019	161.278	39.30	18.37	–	Spring, 2008	Doherty et al. (2010)	22.52	1.33
56	Eastern Russia	69.020	161.279	52.40	31.90	–	Spring, 2008	Doherty et al. (2010)	35.97	1.30
57	Eastern Russia	68.737	161.521	57.70	15.53	–	Spring, 2008	Doherty et al. (2010)	23.89	2.68
58	Eastern Russia	68.719	161.572	53.00	18.00	–	Spring, 2008	Doherty et al. (2010)	24.94	2.23
59	Eastern Russia	68.700	161.623	42.05	8.30	–	Spring, 2008	Doherty et al. (2010)	14.99	2.15
60	Eastern Russia	69.869	169.302	11.00	10.00	–	Spring, 2008	Doherty et al. (2010)	10.20	0.06
61	Eastern Russia	69.782	169.720	11.90	8.07	–	Spring, 2008	Doherty et al. (2010)	8.83	0.24
62	Eastern Russia	68.930	170.713	14.30	9.30	–	Spring, 2008	Doherty et al. (2010)	10.29	0.32
63	Eastern Russia	69.330	170.856	11.50	15.30	–	Spring, 2008	Doherty et al. (2010)	14.55	0.24
64	Eastern Russia	69.119	170.858	14.00	11.00	–	Spring, 2008	Doherty et al. (2010)	11.59	0.19
65	Eastern Russia	69.022	170.918	23.20	10.80	–	Spring, 2008	Doherty et al. (2010)	13.26	0.79
66	Eastern Russia	69.195	170.946	13.20	12.00	–	Spring, 2008	Doherty et al. (2010)	12.24	0.08
67	Eastern Russia	69.571	171.015	9.50	14.88	–	Spring, 2008	Doherty et al. (2010)	13.81	0.34
68	Eastern Russia	69.524	171.310	13.00	13.00	–	Spring, 2008	Doherty et al. (2010)	13.00	0.00
69	Eastern Russia	69.478	171.605	18.00	14.43	–	Spring, 2008	Doherty et al. (2010)	15.14	0.23
70	Western Svalbard	78.910	11.720	–	–	3.20	Mar–Apr, 2007	Forsstrom et al. (2009)	3.20	–
71	Western Svalbard	78.870	12.460	–	–	1.70	Apr, 2007	Forsstrom et al. (2009)	1.70	–
72	Western Svalbard	79.000	14.000	–	–	1.40	Apr, 2007	Forsstrom et al. (2009)	1.40	–
73	Eastern Svalbard	77.897	18.302	–	–	9.80	Mar, 2007	Forsstrom et al. (2009)	9.80	–
74	Eastern Svalbard	78.750	17.580	–	–	6.60	Mar, 2007	Forsstrom et al. (2009)	6.60	–
75	Eastern Svalbard	79.910	25.000	–	–	6.50	Apr, 2007	Forsstrom et al. (2009)	6.50	–
76	Northern Greenland	81.000	301.000	–	–	2.60	Spring, 2008	Doherty et al. (2010)	2.60	–
77	West of Greenland	77.450	299.500	–	–	3.30	Spring, 2008	Doherty et al. (2010)	3.30	–
78	West of Greenland	76.40	292.30	–	–	4.30	Spring, 2008	Doherty et al. (2010)	4.30	–

ACPD
12, 11245–11274, 2012

Table 2. Present-day sBC observations in the Arctic Ocean in summer. The estimated sBC of whole layer at each measurement site is calculated from surface and subsurface BC concentrations with snow densities observed in 3rd Chinese Arctic expedition in summer 2008. All of the sBC measurements in summer are carried out on the surface of Arctic sea ice, they are largely influenced by drifting sea ice. There is almost no obvious snow covering the ice surface, except new snow and material that between snow and ice in some regions. Thus, there are large uncertainties in current analysis, and present observations can only give a general and rough indication to the spatial distribution of sBC in summer. As the initial field of BC deposition, the Arctic Ocean is divided into several latitude zones in this study and each zone is characterized by one value averaged from the observations within this area.

NO.	Lat (°N)	Lon (°E)	surface	subsurface	Whole layer	Measurement period	Reference	Estimated sBC (ng g^{-1})	Uncertainty of Estimation
1	73.7	192.59	–	–	5.7	Jul, 2010	This study	5.7	–
2	73.72	192.72	–	–	6.5	Jul, 2010	This study	6.5	–
3	73.74	193.04	–	–	15.9	Jul, 2010	This study	15.9	–
4	75	200.01	–	–	11.4	Jul, 2010	This study	11.4	–
5	75	202.5	–	–	2.8	Jul, 2010	This study	2.8	–
6	75.02	199.98	–	–	2.9	Jul, 2010	This study	2.9	–
7	75.03	200.52	–	–	7.4	Jul, 2010	This study	7.4	–
8	75.71	222.8	–	–	16	Aug, 2005	U.Vic	16	–
9	75.908	219.411	10.2	10.2	–	Aug, 2008	Doherty et al. (2010)	10.2	0.0
10	75.908	219.411	12.2	8.5	–	Aug, 2008	Doherty et al. (2010)	9.7	0.2
11	75.99	203.05	–	–	41.6	Jul, 2010	This study	41.6	–
12	76	203.97	–	–	10.2	Jul, 2010	This study	10.2	–
13	76.81	199.48	–	–	40.2	Aug, 2010	This study	40.2	–
14	77.04	200.18	–	–	22.1	Aug, 2010	This study	22.1	–
15	77.04	200.18	–	–	9.5	Aug, 2010	This study	9.5	–
16	77.04	200.18	–	–	8.5	Aug, 2010	This study	8.5	–
17	77.702	213.398	10	–	–	Jul, 2008	Doherty et al. (2010)	10.0	–
18	77.9	200.13	–	–	39.2	Aug, 2010	This study	39.2	–
19	77.98	200.36	–	–	29.8	Aug, 2010	This study	29.8	–
20	77.98	200.36	–	–	10.8	Aug, 2010	This study	10.8	–
21	78	220.42	–	–	15	Aug, 2008	Doherty et al. (2010)	15.0	–
22	78.01	209.818	4.2	15.2	–	Aug, 2008	Doherty et al. (2010)	14.3	0.6
23	78.291	183.321	12.3	–	–	Aug, 2005	Doherty et al. (2010)	12.3	–
24	78.387	206.549	21	22.1	–	Aug, 2008	Doherty et al. (2010)	21.6	0.1
25	78.392	206.377	16.4	9.3	–	Aug, 2008	Doherty et al. (2010)	10.9	0.4
26	78.6	216.5	–	–	26	Aug, 2005	U.Vic	26.0	–
27	78.91	11.87	–	–	30.9	Sep, 1985	Clarke et al. (1985)	30.9	–
28	79.8	355.8	–	–	38.7	Jul, 1985	Clarke et al. (1985)	38.7	–
29	79.83	331.21	–	–	1.2	Aug, 2008	Doherty et al. (2010)	1.2	–
30	79.88	333.99	–	–	4.8	Aug, 2008	Doherty et al. (2010)	4.8	–

ACPD
12, 11245–11274, 2012

Table 2. Continued.

NO.	Lat (°N)	Lon (°E)	surface	subsurface	Whole layer	Measurement period	Reference	Estimated sBC ($ng\,g^{-1}$)	Uncertainty of Estimation
31	79.988	209.713	28.9	–	–	Aug, 2008	Doherty et al. (2010)	28.9	–
32	80.003	209.656	49.4	–	–	Aug, 2008	Doherty et al. (2010)	49.4	–
33	80.081	209.792	23.5	13.7	–	Aug, 2008	Doherty et al. (2010)	18.3	0.6
34	80.75	183.21	–	–	20	Aug/Sep, 2008	HOTRAX	20	–
35	81.226	182.805	3.5	–	–	Aug, 2005	Doherty et al. (2010)	3.5	–
36	81.226	182.805	4.1	–	–	Aug, 2005	Doherty et al. (2010)	4.1	–
37	81.6	189.86	–	–	15	Sep, 2008	HOTRAX	15	–
38	81.723	209.035	5.7	8.6	–	Aug, 2008	Doherty et al. (2010)	7.2	0.2
39	81.926	210.071	14.1	–	–	Aug, 2008	Doherty et al. (2010)	14.1	–
40	81.997	219.943	4.3	17.7	–	Aug, 2008	Doherty et al. (2010)	14.4	0.8
41	83.087	185.329	3	–	–	Aug, 2005	Doherty et al. (2010)	3.0	–
42	83.087	185.329	4.3	–	–	Aug, 2005	Doherty et al. (2010)	4.3	–
43	83.299	188.112	1.8	–	–	Aug, 2005	Doherty et al. (2010)	1.8	–
44	83.299	188.112	5.2	–	–	Aug, 2005	Doherty et al. (2010)	5.2	–
45	83.955	216.808	4.2	–	–	Aug, 2005	Doherty et al. (2010)	4.2	–
46	83.955	216.808	11.8	–	–	Aug, 2005	Doherty et al. (2010)	11.8	–
47	84.171	209.005	2.6	–	–	Aug, 2005	Doherty et al. (2010)	2.6	–
48	84.171	209.005	7	–	–	Aug, 2005	Doherty et al. (2010)	7.0	–
49	84.23	206.42	–	–	9	Aug, 2008	HOTRAX	9	–
50	84.307	210.918	4.6	–	–	Aug, 2005	Doherty et al. (2010)	4.6	–
51	84.309	199.352	2	–	–	Aug, 2005	Doherty et al. (2010)	2.0	–
52	84.309	199.352	14.4	–	–	Aug, 2005	Doherty et al. (2010)	14.4	–
53	84.311	199.581	2.2	–	–	Aug, 2005	Doherty et al. (2010)	2.2	–
54	84.311	199.581	15.7	–	–	Aug, 2005	Doherty et al. (2010)	15.7	–
55	85.122	205.2	18.8	–	–	Sep, 2005	Doherty et al. (2010)	18.8	–
56	85.938	48.335	6.4	2.8	–	Sep, 2005	Doherty et al. (2010)	4.5	0.2
57	85.938	48.335	9.6	–	–	Sep, 2005	Doherty et al. (2010)	9.6	–
58	86.04	197.34	–	–	5	Sep, 2008	HOTRAX	5	–
59	86.657	55.618	3.7	6.1	–	Sep, 2005	Doherty et al. (2010)	5.0	0.1
60	87.472	57.588	4.2	9.6	–	Sep, 2005	Doherty et al. (2010)	7.1	0.3
61	87.62	155.876	2.7	–	–	Sep, 2005	Doherty et al. (2010)	2.7	–
62	87.62	155.876	30	–	–	Sep, 2005	Doherty et al. (2010)	30.0	–
63	87.66	150.902	8	–	–	Aug, 2005	U.Vic	8.0	–
64	88.056	58.748	2.3	2.1	–	Sep, 2005	Doherty et al. (2010)	2.2	0.0
65	88.456	146.532	5.3	–	–	Sep, 2005	Doherty et al. (2010)	5.3	–
66	88.456	146.532	22.4	–	–	Sep, 2005	Doherty et al. (2010)	22.4	–
67	88.46	213.47	7	–	–	Aug, 2005	U.Vic	7.0	–
68	88.813	164.136	18.2	–	–	Sep, 2005	Doherty et al. (2010)	18.2	–
69	88.813	164.136	1.7	–	–	Sep, 2005	Doherty et al. (2010)	1.7	–
70	89.374	270.912	2.7	13.3	–	Sep, 2005	Doherty et al. (2010)	8.4	0.6
71	89.482	169.798	7.1	2.3	–	Sep, 2005	Doherty et al. (2010)	4.5	0.3

ACPD
12, 11245–11274, 2012

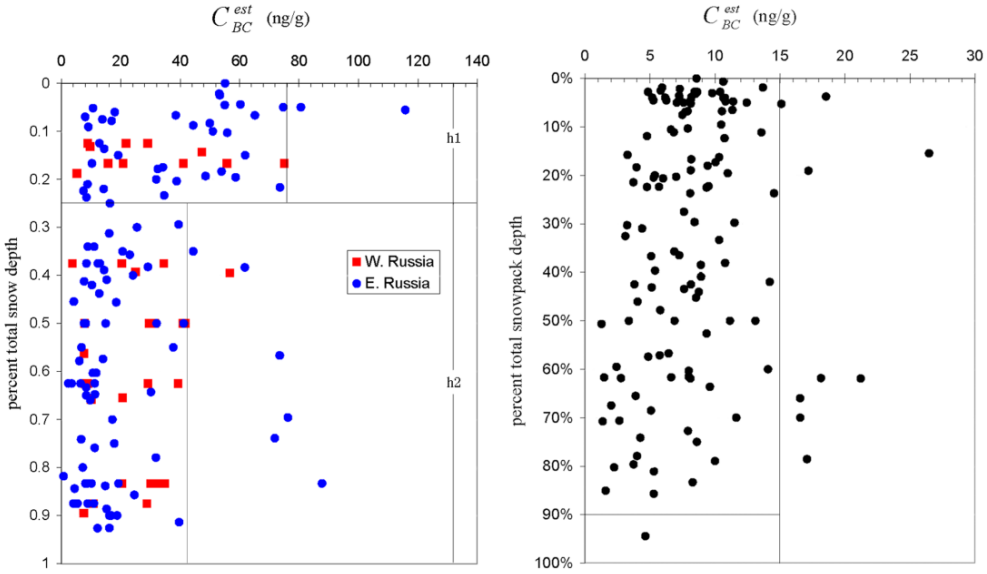

Fig. 1. Vertical profile of sBC concentrations in the Arctic snow from the field measurements in west (2007) and east (2008) Russia (left), and profile from the field measurements in Canada in spring 2009 (right). C_{BC}^{est} denotes the estimated true mass of BC per mass of snow. These two figures are respectively from Figs. 12a and 9 (left panel) in Doherty et al. (2010), but with some necessary modifications to highlight different concentrations of sBC in various depths.

ACPD
12, 11245–11274, 2012

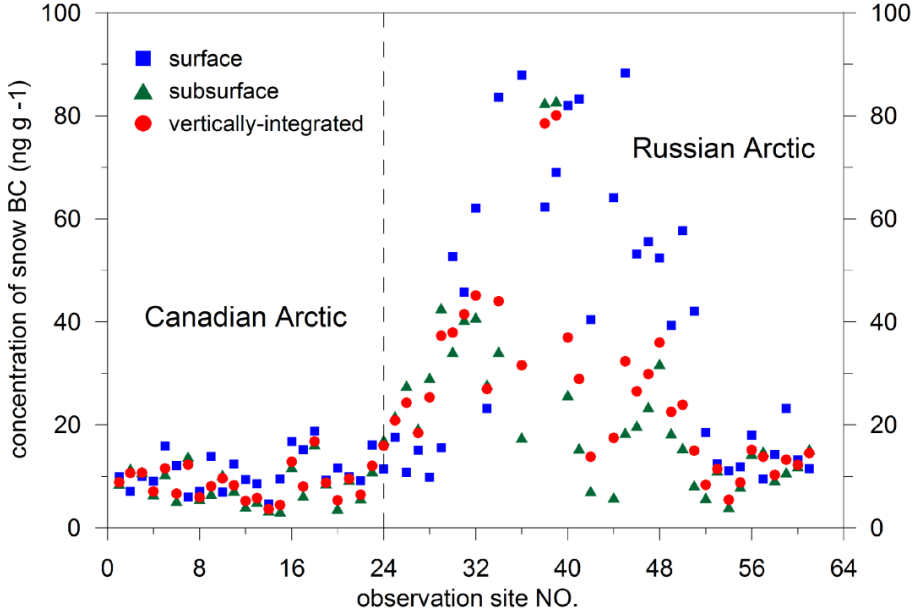

Fig. 2. Present observations of surface (blue), subsurface (green) and whole-layer (red) sBC in the Canadian and Russian Arctic north of 66° N. Observations in Canadian Arctic and Russian Arctic are separated by a dash line, The values larger than 70 ng g^{-1} are excluded in this study because of too large difference between surface and subsurface concentrations shown in these sites, which may bring great uncertainties.

ACPD
12, 11245–11274, 2012

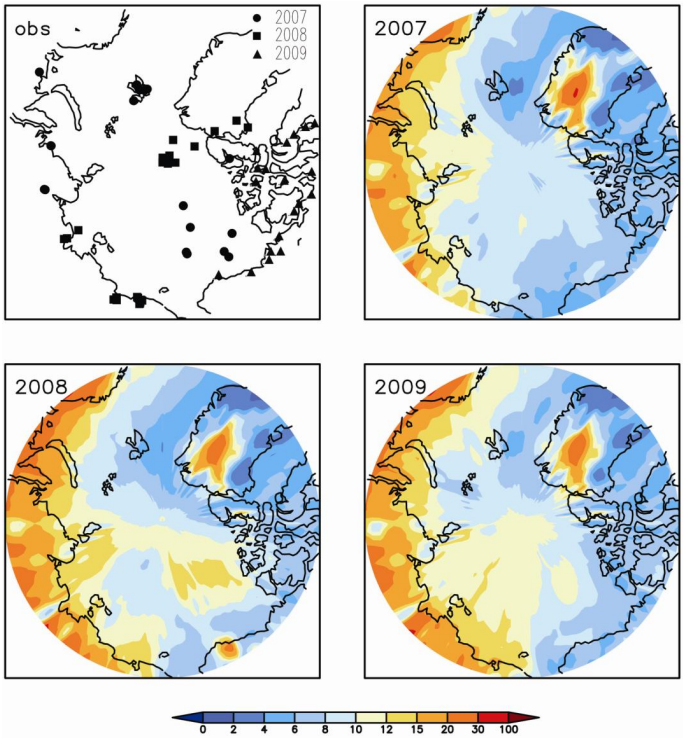

Fig. 3. Present sBC measurements in and around the Arctic Ocean in spring 2007–2009 (scattered) and the spatial distribution of modeled sBC in corresponding period (shaded). In the scatter diagram, different marks denote different measurement years.

ACPD
12, 11245–11274, 2012

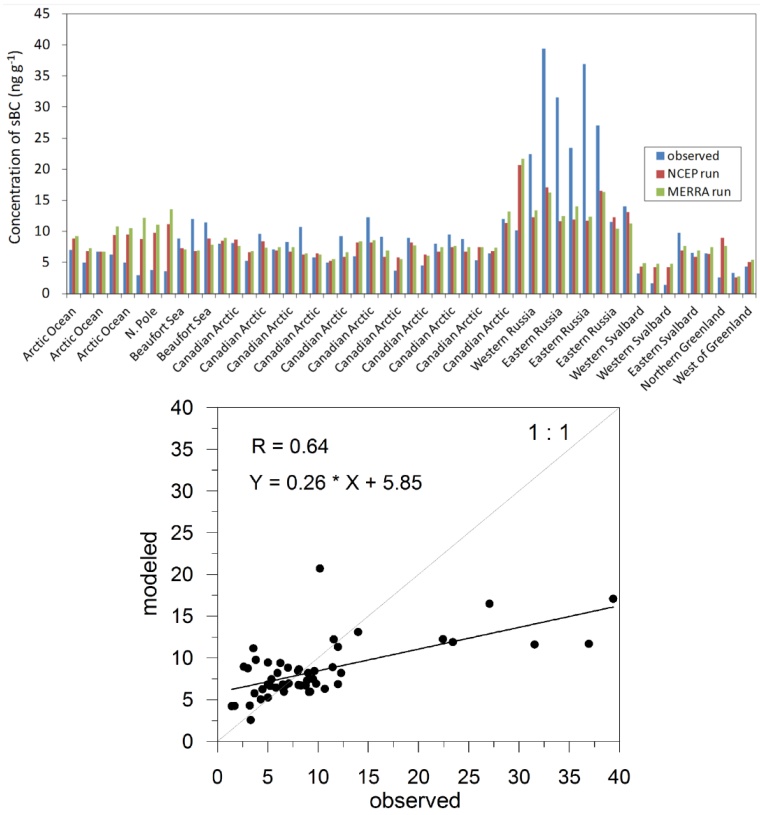

Fig. 4. Histogram (upper) and scatterplots (bottom) of modeled versus observed sBC content for the Arctic Ocean and surrounding regions in spring 2007–2009. Model results are sampled for the month and year of observations and interpolated to corresponding measurement sites. The modeled sBC from NCEP and MERRA runs are both shown in the histogram and 1 : 1 line is also shown in scatterplots.

ACPD
12, 11245–11274, 2012

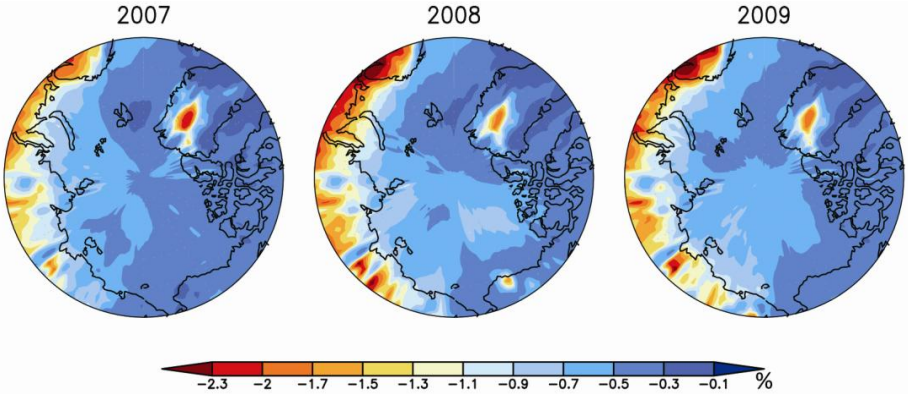

Fig. 5. Modeled decrease in snow and ice albedo due to sBC in and around the Arctic Ocean (north to 66° N) in spring 2007–2009.

ACPD
12, 11245–11274, 2012

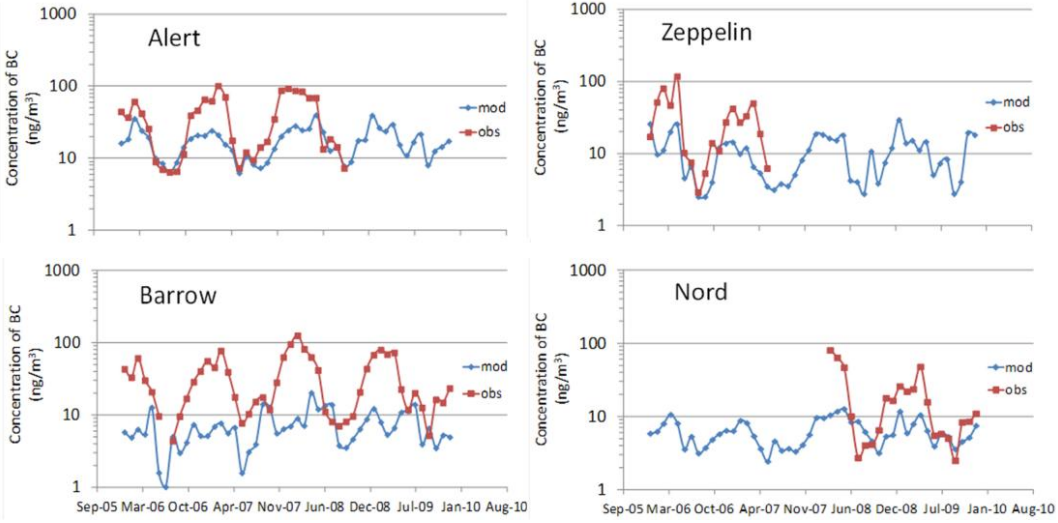

Fig. 6. Comparison of modeled monthly aBC concentrations in near surface layer versus measured concentrations for Alert (83° N, 62° W), Barrow (71° N, 157° W), Zeppelin (79° N, 12° E) ana Nord (81° N, 16° W) station from January 2006 to December 2009.

ACPD
12, 11245–11274, 2012